Applied Physics B (2022) 128:79
https://doi.org/10.1007/s00340-022-07789-9

Applied Physics B
Lasers and Optics

An effective holographic amplifier exploiting consistent periodic structures

S. Bugaychuk[1] · O. Gnatovskiy[1] · P. Yezhov[1] · A. Negriyko[1] · V. Gnatovskyy[2] · A. Sidorenko[3]

Received: 23 November 2021 / Accepted: 24 February 2022 / Published online: 24 March 2022

Abstract
The energy transfer between interacting laser beams is known as the remarkable effect of self-action of coherent waves in nonlinear optics. We demonstrate both experimentally and theoretically that such an effect can be obtained in a holographic setup based on a permanent phase dual-grating. We have found a new mode of unidirectional energy transfer from a strong pump beam to a weak signal beam, achieved through their diffraction on a set of two matched thin gratings. A theoretical description of this effect is developed based on a system of coupled waves and the formalism of generation of a shifted (nonlocal) dynamic grating with a spatially localized amplitude due to wave-mixing inside a bulk medium. Under the condition of a decrease in the intensity of a weak signal beam, the theory predicts almost complete energy transfer with a diffraction efficiency of ~ 100 % from a stronger pump beam. This unidirectional mode is realized in a thick dual-grating with high modulation depth and cannot be achieved during self-action process of wave-mixing in nonlinear media. The obtained results open the way to design a new type of optical amplifiers and optical phase conjugation systems with great efficiency for amplifying weak signals.

1 Introduction

Optical amplifiers, which exploit wave interaction in nonlinear media, are widely used photonic devices. The most famous of them, optical parametric amplifiers, are based on the interaction of waves of different frequencies and on the transfer of energy from the fundamental harmonic beam to the high harmonic beams [1, 2]. At the same time, the amplification of weak signals of the fundamental frequency is required in many specific tasks, for example, in lidar systems or for optical phase conjugation [3–5]. A successful approach to effective amplification of laser beams in modern technologies is the use of large distances for mixing laser beams in optical fibers [2, 6, 7].

Alternatively, the effect of energy transfer between two coherent waves resulting from their mixing in a nonlinear medium been seen as a valid method for this purpose [8, 9]. In this case, the energy exchange conditions are obtained in the Bragg regime, which is implemented in a bulk nonlinear optical media for two incident beams (pump and signal). Bragg diffraction by a regular grating became valid for many experimental techniques, such as X-ray diffraction [10, 11], acousto-optic modulators, the study of neutron or electron scattering [12]. The Pendellösung phenomenon, which exhibits as the exchange of energy between diffracted and direct beams due to constructive and destructive interference of waves, is highlighted in the dynamic theory of diffraction (see, e.g. [13–15]). The Pendellösung phenomenon manifests itself as a dependence of the intensity of a diffracted wave on parameters that affect its phase change, for example, changing the thickness of the medium or monitoring the direction of propagation of input waves. The formation of a dynamic grating in the case of two-beam coupling refers to the processes of self-action occurring in a nonlinear dynamic medium, therefore, it has some peculiarities. The first relates to self-diffraction, which is that when two input beams form a light interference pattern (light lattice), it generates a periodic structure of photoinduced refractive index (or/and photoinduced absorption), i.e. a dynamic grating, inside an optically nonlinear medium, for

✉ S. Bugaychuk
bugaich@iop.kiev.ua

[1] Institute of Physics of National Academy of Sciences of Ukraine, 46 Prospect Nauki, Kyiv 03028, Ukraine

[2] Faculty of Physics, Taras Shevchenko National University of Kyiv, 4 Prospect Hlushkova, Kyiv 03127, Ukraine

[3] Kyivmetroproekt LLC, 16/22 Bohdana Khmelnytskogo Str., Kyiv 01030, Ukraine

example, in a photorefractive crystal. During this process, the recording beams are diffracted by the dynamic grating created by them. Secondly, both gratings, the light lattice and the dynamic grating, have the same spatial period . The process of self-diffraction is described by the coupled-wave equations derived from the wave equation for the total field, which is a superposition of two coherent plane waves [16]. These equations indicate the phase shift that a wave gets due to diffraction from the dynamic grating. Thus, if the dynamic grating is local, i.e. the maxima of the dynamic grating coincide with the maxima of the interference pattern, there is no energy transfer between the interacting beams, but only a phase transfer as a result of the self-diffraction process. However, an effect similar to the Pendellösung phenomenon will be observed when two lattices are mutually displaced relative to each other [8, 9, 17]. Since the phase delay is acquired in the changed propagation path, as well as constructive and destructive interference between the diffracted and direct waves, an oscillatory behavior of the intensities in the output Bragg beams is observed. When a mutually shift is made within the spatial period Λ, the maximum output intensity will be observed at $\Lambda/4$ spatial shift, which corresponds to phase delay of $\pi/2$. Let's denote the diffracted wave as a "signal" with input intensity I_{s0} and the direct wave as a "pump" with the input intensity I_{p0}. The maximum energy transfer and amplification of the signal beam will be observed when the dynamic grating is shifted relative to the light lattice by $\Lambda/4$ in the direction of signal wave propagation due to the constructive interference between the diffracted and direct beams. This is the so-called "direct" energy transfer from the pump beam to the signal one. And vice versa, if the dynamic grating is shifted in the direction of the pump wave, $-\Lambda/4$, there is a "reverse" energy transfer from the signal beam to the pump. A similar energy transfer in Bragg orders was obtained using constant thick holographic gratings when illuminated by an interference light pattern and with its spatial displacement relative to the grating [18].

The exchange of energy occurs due to self-diffraction of two laser beams on a nonlocal dynamic phase grating formed by the same beams in the nonlinear medium is the subject of strong interest in dynamic holography. Theoretically, the complete (100%) energy transfer from the pump beam to the signal beam is predicted with wave-mixing in a bulk photorefractive medium [19, 20]. But the practical implementation of such an effect turned out to be very limited, associated with the significantly small amplitude of the registered dynamic grating (Δn), which is usually $10^{-4} \div 10^{-6}$ in magnitude. In addition, with a large difference in the intensities of the pump and signal beams, the contrast of their interference pattern becomes almost invisible, which leads to an insignificant modulation depth of the recorded dynamic grating formed by this light contrast.

In our study, we propose to overcome this drawback by simulating a stationary dynamic grating in a bulk medium using a set of phase permanent gratings (a dual-grating of a special design having a layer of space), which is consistent with the light interference pattern formed by the pump and signal beams. We have shown that, owing to a layer of space, such a set of thin gratings supports the Bragg condition for diffraction of waves. Theoretically and experimentally, we have found that in the case of a small modulation depth for both gratings, an energy exchange traditional for nonlinear media occurs, namely, two cases: direct energy transfer (from the pump beam to the signal beam) and reverse energy transfer (from the signal beam to the pump beam), which are determined by the direction of the displacement of this thick dual-grating relative to the light interference pattern. But when the both gratings have a large modulation depth, we get a new unknown mode: only a weak beam is always amplified, regardless of the shear direction of the thick dual-grating. We provide a theoretical explanation of this phenomenon. We perform the first experimental observation of energy transfer in a holographic set-up based on a thick dual-grating we made. These studies confirm the existence of two different modes of energy transfer depending on the values of the modulation depth of the phase gratings.

2 Basic optical scheme of a holographic amplifier with a thick dual-grating

The efficiency of energy transfer between two interacting waves in a nonlinear medium is determined by the coupling strength $\Gamma = k\gamma_N d$, where $k = 2\pi/\lambda$ is the wave vector, d is the thickness of the medium, and $\gamma_N = \Delta n$ is the maximum amplitude of the nonlocal dynamic grating [16, 21]. Typical values for the observed energy exchange in photorefractive crystals should be $\Gamma \approx 5 \div 10$ (see, for example, [8, 9, 22]). That requires a sufficiently large crystal thickness: $d \approx 5 \div 10$ mm for $\Delta n = 10^{-4}$, or $d > 50$ mm for $\Delta n = 10^{-5}$ (for $\lambda = 633$ mm).

In this section, we prove that a thick stationary dynamic grating in such an extended medium can be successfully replaced by a set of thin matched gratings separated by layers of space. The basic scheme with a set of two gratings is shown in Fig. 1. It represents a traditional Fourier transform scheme, but the working area includes two separated holographic gratings. Transformation of the input interference pattern, which is formed by the pump I_{p0} and a signal I_{s0} beams, by two gratings is fixed in the far zone (in the Fourier plane of the lens). We study the intensity changes in the two main diffraction orders at the output.

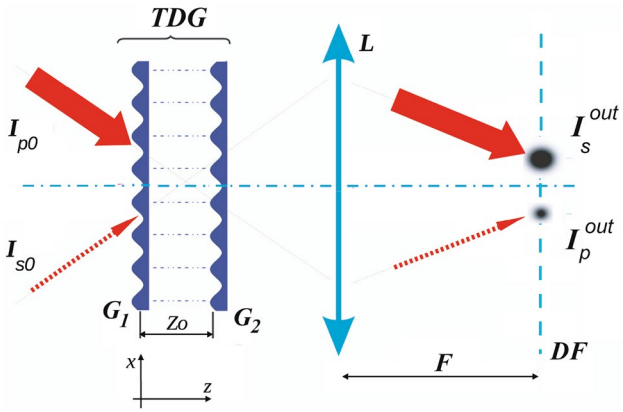

Fig. 1 The principal optical scheme of coupled beams with two gratings. *TDG* shows a set of two matched gratings, G_1 and G_2 are thin phase gratings, L is the lens, F is the focal length of the lens, Z_0 is the distance between the gratings, I_{s0} and I_{p0} are the input intensities of the signal and pump beams, I_s^{out} and I_p^{out} are the output intensities of the signal and pump beams, respectively, *DF* is Fourier plane registering diffraction orders

Further, we prove that two thin phase gratings, G_1 and G_2, separated from each other by a distance Z_0, can, under certain conditions, simulate Bragg diffraction. The two matched gratings should have the same period (Λ) and they should not be offset from each other in the transverse direction. Therefore, we introduce the following notation for the thick dual-grating (TDG). To satisfy the Bragg diffraction, two conditions must be fulfilled. Firstly, the spatial period of the interference pattern (Λ_{int}) should be a multiple of the period of the thin gratings. Secondly, the interference pattern of the input light must be shifted relative to the *TDG* in the transverse direction x. The features of beams' transformation in such a system are demonstrated in Fig. 2. The figure shows the intensity distributions calculated in the output diffraction orders at different input configurations. We have chosen both gratings with a large modulation depth, which gives a phase delay for each grating $\Phi_1 = \Phi_2 = 1$, as well as a large distance between the gratings $Z_0 = 50$ mm. Calculations are based on scalar diffraction theory [23, 24]. (Note, that the definition of the phase delay of a thin holographic grating $\Phi = k\Delta nd$ formally coincides with the formula for the coupling constant of two-wave interaction in the steady state Γ.)

Figure 2a shows the intensity spectrum in diffraction orders when only single probe beam is at the input normal to the *TDG*. The spectrum is equivalent to the diffraction of a beam on one thin phase grating, the modulation depth of which is summed by two gratings in the *TDG*. It consists of the main strong order (denoted as {0}) and high diffraction

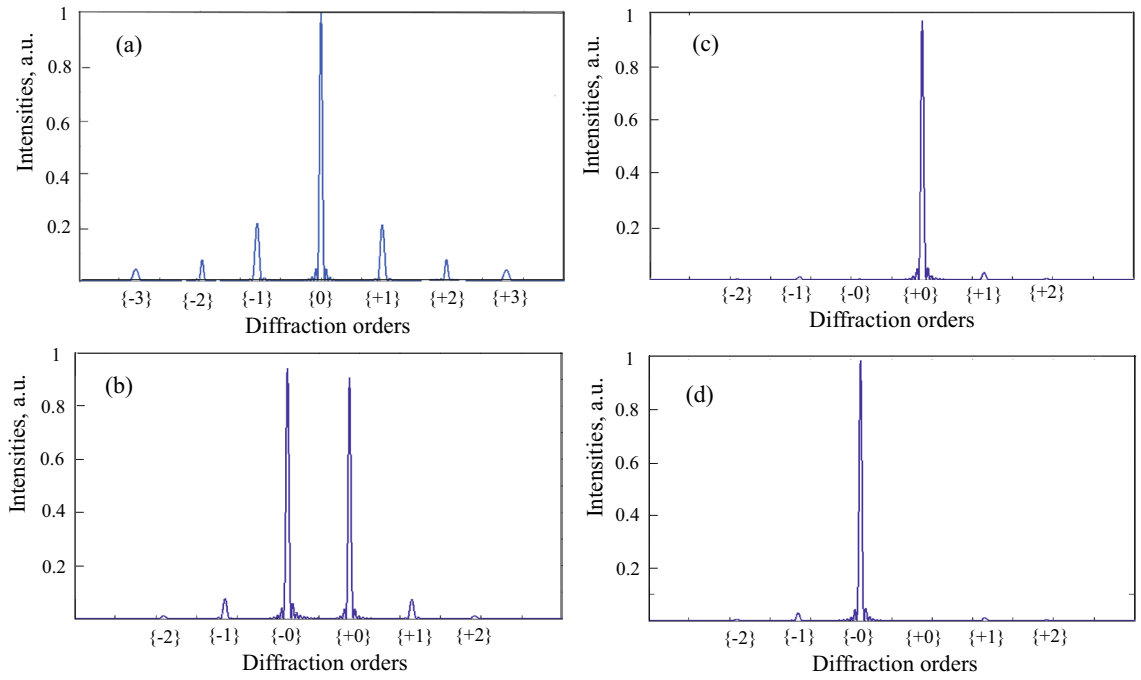

Fig. 2 Calculations the distribution of the intensities in output diffraction orders for different input conditions in the optical scheme, which is shown in Fig. 1: **a** a single pump beam I_{p0} enters normally to *TDG*; **b** both the signal beam and the pump beam are at the input with the same intensities, there is no mutual shift between the interference pattern and *TDG* ($\delta = 0$); **c** "direct" energy transfer due to the spatial shift between the interference pattern and *TDG*, $\delta = 0.25\,\Lambda$; **d** "reverse" energy transfer in the case of $\delta = 0.75\,\Lambda$. The parameters of the scheme are as follows: $Z_0 = 50$ mm, G_1 and G_2 have the same modulation depth, which gives a phase delay $\Phi_1 = \Phi_2 = 1$ rad, $I_{s0} = I_{p0}$, $\Lambda_{int} = 2\Lambda$

orders, which have the same intensities in symmetric orders [25]. When two coherent beams are at the input (Fig. 2b), the intensity spectrum changes. It includes two main diffraction orders corresponding to two recording beams, which we define by analogy with the diffraction of a single input beam as $\{-0\}$ and $\{+0\}$, as well as high diffraction orders. The main diffraction orders $\{-0\}$ and $\{+0\}$ correspond to the Bragg orders in the case of diffraction on a thick grating. In our notation, we use the output "pump" beam for the order $\{-0\}$ and output "signal" beam for the orders $\{+0\}$.

As a rule, during diffraction on a thin phase grating, a rather large part of the total input intensity is distributed to high diffraction orders at the output. The Bragg-like condition can be satisfied when there exists a shift of the interference pattern with respect to the *TDG*. Just due to this shift, energy is mostly redistributed between the two main diffraction orders, $\{-0\}$ and $\{+0\}$. At the same time, high diffraction orders take off a small fraction of the total intensity. In the case of spatial shift ($\delta = +\Lambda/4$) of maximums of the interference pattern in the direction of gratings' minimums, only one signal beam is greatly enhanced, I_s^{out}. This case is called direct energy transfer. The others diffraction orders almost vanish (Fig. 2c). If the spatial shift occurs in the opposite direction ($\delta = -\Lambda/4$), the only pump beam is significantly amplified at the output, I_p^{out}, and all other diffraction orders almost disappear, (Fig. 2d). This is a case of reverse energy transfer.

3 Modeling of energy exchange at two-wave coupling in an extended medium

We consider the analytical solutions of two-wave coupling in an extended nonlinear medium under the assumption that the medium has a purely nonlocal response. In this case, both the input interference light pattern, which is formed by two coupled waves, and the photoinduced dynamic grating have a sinusoidal profile along the transverse direction x, but they are mutually shifted by a quarter of the grating period. Then the energy transfer occurs between the two coupled waves that leads to a change in their mutual intensities over the thickness of the medium z. This process results in a change in the contrast of the light interference inside the medium. Modeling of such a process is based on the coupled-wave theory. The changes in the amplitudes of two coupled waves during their propagation in a dynamic nonlinear medium are described by the following system [8, 16, 26]:

$$\frac{\partial \mathbf{E}_s(z)}{\partial z} = kN(z)\mathbf{E}_p(z)\ ; \quad \frac{\partial \mathbf{E}_p^*(z)}{\partial z} = -kN(z)\mathbf{E}_s^*(z) \tag{1}$$

where $N(z)$ denotes the amplitude of the nonlocal dynamic grating, $z/(\pm\cos\theta)$ is the direction of wave propagation, and here we take into account that the angle of convergence of the two waves, θ, small, so $\cos(\theta) \simeq 1$.

The analytical solutions of the system (1), which relate the intensities of the waves at the input and output, have been reported in numerous publications for photorefractive materials that cover many important situations of experimental beam coupling (see, for example, [9, 19–21, 26, 27]). These solutions were obtained under the assumption that the light contrast remains constant over the thickness z. We will consider the case of varying the light contrast in the volume of the medium. This leads to a change in the amplitude of the photoinduced grating $N(z)$ along the thickness z. The dependence of the grating amplitude on the light intensity is taken from the evolution equation (see [28–32]):

$$\frac{\partial N(z)}{\partial t/\tau} = \gamma_N J_m - N(z) \tag{2}$$

where γ_N is a dimensionless quantity determining the maximum possible amplitude of the shifted (nonlocal) grating, τ is the relaxation constant of the grating amplitude, and the term $J_m = (\mathbf{E}_s\mathbf{E}_p^* + \mathbf{E}_s^*\mathbf{E}_p)/I_0$ describes the light contrast inside the medium, where $I_0 = I_s + I_p = \text{const}$ in the transmission geometry under condition to neglect of the absorption in the medium ($I_i = \mathbf{E}_i\mathbf{E}_i^*,\ \mathbf{E}_i = E_i e^{\varphi_i},\ i = s, p$). We use the approach in which we first obtain a solution for the distribution of the grating amplitude $N(z)$, and then the output intensities will be expressed through this solution. For the steady state ($\partial N(z)/\partial t = 0$), the system (1)–(2) can be rewritten in new variables $N(z)$, $J_m(z)$ and $J_d(z) = (\mathbf{E}_p\mathbf{E}_p^* - \mathbf{E}_s\mathbf{E}_s^*)/I_0$:

$$N(z) = \gamma_N J_m(z)\ ; \tag{3}$$

$$\frac{\mathrm{d}J_m^2}{\mathrm{d}z} = 4k\gamma_N \cdot J_d J_m^2\ ; \qquad \frac{\mathrm{d}J_d}{\mathrm{d}z} = -2k\gamma_N \cdot J_m^2 \tag{4}$$

Dividing the first equation by the second in (4), we get the first integral of the system:

$$C^2 = J_m^2 + J_d^2 = I_s I_p/I_0^2 + (I_p - I_s)^2/I_0^2 = \text{const} \tag{5}$$

Using the definition of C^2, we can integrate the first equation in (4) and find a solution for $J_m(z)$. Then applying (3) the amplitude profile of the grating will take the following form:

$$N(z) = \frac{\gamma_N C}{\cosh(2\gamma_N C \cdot kz - q)} \tag{6}$$

where both the constants C and the integration constant q are determined by the input intensities at the boundary of

the medium. The formula (6) shows that in the steady state the spatial profile of the grating amplitude takes on a localized soliton-like form. Both the degree of localisation of the soliton-like profile of the $N(z)$ and the location of its maximum are determined by two parameters: the maximum amplitude γ_N and the ratio of the input wave intensities.

Knowing the spatial distribution of the grating amplitude $N(z)$, we can determine the output intensities, wich are expressed as an integral over $N(z)$ within the boundaries of z_1 and z_2 of the medium ([31, 32]). To do this, we rewrite the system (1) for the amplitudes and phases of the waves:

$$\begin{aligned} \frac{\mathrm{d}E_s}{\mathrm{d}z} &= kN(z)E_p\ \cos(\varphi_{sp})\ ; \quad \frac{\mathrm{d}E_p}{\mathrm{d}z} = -kN(z)E_s\ \cos(\varphi_{sp})\ ; \\ \frac{\mathrm{d}\varphi_{sp}}{\mathrm{d}z} &= kN(z)\frac{E_p^2 - E_s^2}{E_s E_p}\sin(\varphi_{sp}) \end{aligned} \tag{7}$$

where $\varphi_{sp} = \varphi_s(z) - \varphi_p(z)$. This system has the first integral $D = E_s E_p \sin(\varphi_{sp}) = \text{const}$, so we can find $\cos(\varphi_{sp}) = \sqrt{E_s^2(I_0 - E_s^2) - D^2}/(E_s E_p)$. Introducing this value of $\cos(\varphi_{sp})$, we can combine the first two equations in (7) in the following integral equation:

$$\begin{aligned} s_{[s,p]} \int\limits_{I_{[s,p]}(z_1)}^{I_{[s,p]}(z_2)} \frac{\mathrm{d}I_{[s,p]}}{\sqrt{-I_{[s,p]}^2 + I_0 I_{[s,p]} - D^2}} \\ = 2k \int\limits_{z_1}^{z_2} N(z)\mathrm{d}z \end{aligned} \tag{8}$$

where one need to choose either I_s and the sign $s_s = 1$, or I_p with $s_p = -1$. We denote the right-hand side in (8) by $U_d = 2k\int_{z_1}^{z_2} N(z)\mathrm{d}z$, which has the physical meaning of the area under the profile of the grating amplitude within the boundaries of the nonlinear medium. Substituting here the solutions (6), we find:

$$\begin{aligned} U_d &= 2\arctan\frac{e^{\chi_2} - e^{\chi_1}}{1 + e^{\chi_1 + \chi_2}}\ , \\ \chi_1 &= 2k\gamma_N C z_1 - q\ , \quad \chi_2 = 2k\gamma_N C z_2 - q \end{aligned} \tag{9}$$

Then the solutions for the output intensities are:

$$\frac{I_s^{\text{out}}}{I_0} = \frac{1}{2}\sin\left[\pm U_d + \arcsin\left(2\frac{I_{s0}}{I_0} - 1\right)\right] + \frac{1}{2} \tag{10}$$

$$\frac{I_p^{\text{out}}}{I_0} = \frac{1}{2}\sin\left[\mp U_d + \arcsin\left(2\frac{I_{p0}}{I_0} - 1\right)\right] + \frac{1}{2} \tag{11}$$

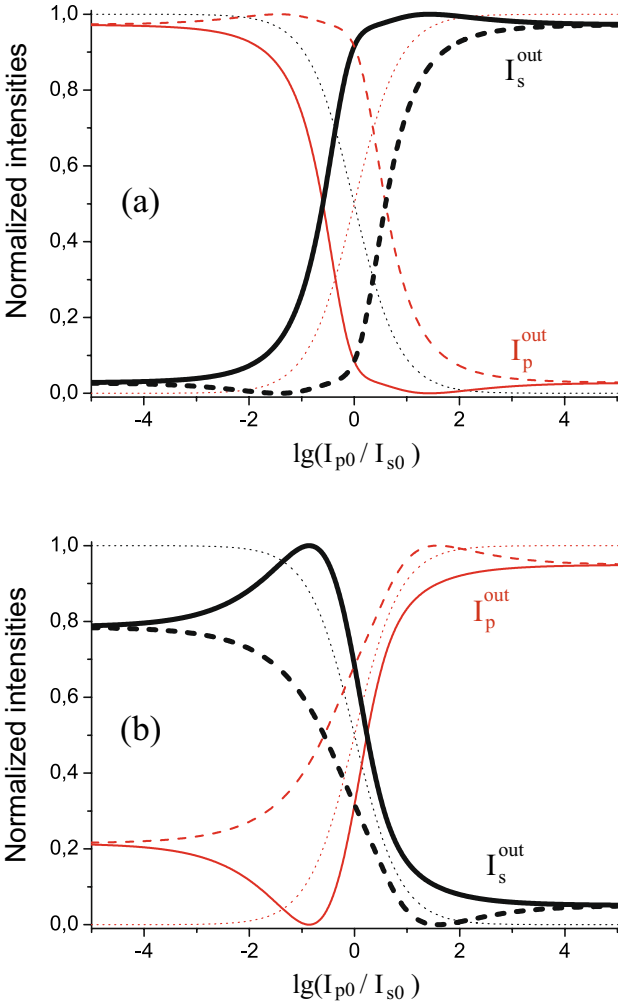

Fig. 3 Theoretical calculations of energy transfer between two coupled waves under Bragg conditions in a bulk medium for different maximum amplitudes of a stationary dynamic grating: **a** $\gamma_N = 5 \cdot 10^{-6}$; **b** $\gamma_N = 5 \cdot 10^{-7}$. Both cases for the sign before U_d in the Eqs. (10)–(11) are plotted: solid lines are for the upper sign, and dash lines for the lower sign; dotted lines for the input intensities. Initial parameters of the optical system: $I_0 = I_{p0} + I_{s0} = 1$, $z_2 - z_1 = 50$ mm, $q = 0$. Black lines for the signal beam, red lines for the pump beam

In formulas (10)–(11), the upper sign before U_d is taken for the case of direct energy transfer, and the lower one is for the reverse energy transfer.

The calculations of the energy transfer according to the formulas (9)–(11) in a wide range of the input intensity ratio are shown in Fig. 3. The curves are plotted in a coordinate system in which the input intensity of the signal beam decreases and the input pump beam increases in the positive direction of the abscissa axis. In the indicated normalization, these curves correspond to diffraction efficiencies,

which we define as follows: $\eta_s = I_s^{\text{out}}/(I_s^{\text{out}} + I_p^{\text{out}})$ for the signal wave; $\eta_p = I_p^{\text{out}}/(I_s^{\text{out}} + I_p^{\text{out}})$ for the pump wave, and $I_s^{\text{out}} + I_p^{\text{out}} = I_0 = 1$.

Figure 3 shows that we have obtained two different modes of energy transfer depending on whether the maximum amplitude γ_N of the photoinduced grating is weak or strong. In the case of strong γ_N, the theory predicts the complete ($\sim 100\%$) energy transfer from the pump beam to the signal one. Moreover, a monotonic increase of the signal intensity occurs for the entire range of the input intensity ratio (see Fig. 3a). The explanation of this result is related to the value of the total phase delay U_d of the generated dynamic grating which depends on the value of γ_N, as follows from (6). For a weak value of γ_N, the value $U_d \le \pi/2$. Moreover, the degree of localization of the grating is small. The grating has a small amplitude and an almost uniform profile over the thickness of the medium. According to formulas (10)–(11), there is a traditional behavior of energy exchange: an increase of the signal intensity for the case of direct energy transfer, and a decrease of the signal intensity accompanied by an increase of the pump intensity during the reverse energy transfer (see Fig. 3b). When γ_N is strong, the grating localization becomes more pronounced in an extended medium. The magnitude of U_d is increased to π: $U_d \to \pi$, and then $\sin(U_d)$ changes its sign in the formulas (10)–(11). As a result, a new mode appears which represents an unidirectional energy transfer. In this case, the intensity of a weaker signal beam always increases regardless of the sign in front of U_d. In Fig. 4 shows the change in the absolute values of the output signal intensity with a decrease in I_{s0} and a strong constant input pump intensity I_{p0}.

The appearance of asymmetric profiles of the output intensities at $I_{s0} \approx I_{po}$ requires additional research. We only note that a significant asymmetry is observed when the total

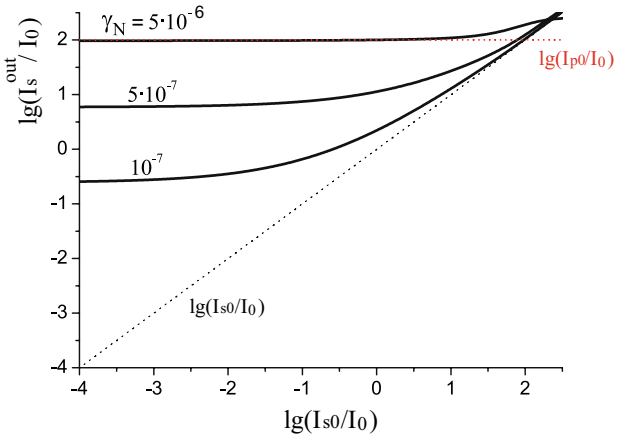

Fig. 4 Normalized output intensity of the signal beam depending on the intensity of the input signal and the amplification coefficient for a strong input pump beam $I_{p0}/I_0 = 200$. The rest of the initial parameters are the same as in Fig. 3; case $+U_d$

phase delay is $U_d \to \pi/2$ due to diffraction on the grating (or, more generally, in the resonances when $U_d \to n \cdot \pi/2$, n-integer). The asymmetry of the profile, along with the interference many waves to form separate independent channels, indicates a similarity with the Fano effect. Similar asymmetric resonant profiles are observed for Fano effects resulting from the interference of (at least two) wave processes, in particular, in the case of wave interference in nanostructures [33, 34]. There are two inherent features of Fano resonance for *TDG*, such as destructive interference and asymmetric resonance profile. The same applies to the suppression of orders with different (multiple) spatial frequencies, shown in Fig. 2. Such suppression can be associated with destructive interference and relates to arising the Fano resonance. The similar was observed in the interaction of several chains of atoms, or guided resonances for transmitted light in photonic crystals [33, 35, 36]. Revealing Fano effects for our system deserves additional research.

Note that our calculations were made under the assumption that the maximum of the grating amplitude is located in the middle of the extended medium ($q = 0$) and does not change its position with varying the input intensity ratio. That is, in this calculation $z_1 = -25$ mm, $z_2 = 25$ mm for the thickness of the medium $Z_0 = 50$ mm. In real dynamic photorefractive media, when the mutual intensities of the input waves change, not only the degree of localization of the grating changes, but also its maximum changes its location along z-axis [31, 32, 37]. An exception is four-wave mixing with four equal input intensities $I_1(z_1) = I_2(z_1) = I_3(z_2) = I_4(z_2)$ or symmetric intensity ratio at the input boundaries: $I_1(z_1)/I_2(z_1) = I_4(z_2)/I_4(z_2)$. Moreover, it can be shown that the value of U_d can not exceed π in the case of a dynamic grating recording during self-diffraction in a bulk nonlinear medium. Thus, our calculations are made formally and correspond to some kind of artificial case. But in the following sections, we will show that such a case can be realized in the system of a thick dual-grating presented in Fig. 1.

4 Experimental study of energy transfer in the holographic amplifier

We experimentally studied the energy transfer between two laser beams at a holographic system with a thick dual-grating. An experimental layout is shown in Fig. 5. Laser beam with $\lambda = 632.8$ nm divided by beam splitter *Bs* on two beams, each of them paths through of the digital grids DG_1 and DG_2, which form two incident beams with the intensities I_{p0} and I_{s0} and the convergence angle 2θ between them. Digital phase gratings were produced by the SLM. Fresnel rhomb *RFr* and analyzer *A* providing the phase operating mode of the SLM. Changing of the phase modulation of DG_2

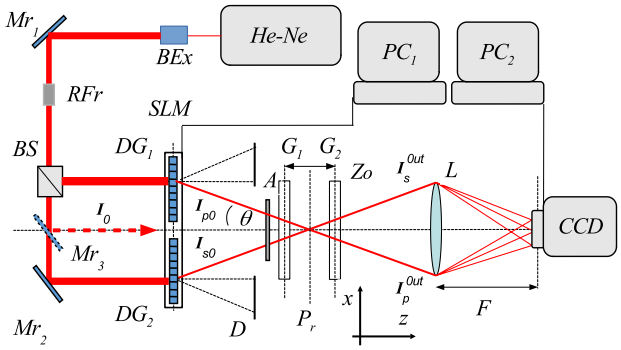

Fig. 5 Optical holographic set-up containing *TDG* for experimental study of energy transfer between two coherent waves: laser—He–Ne laser (632.8 nm); *BEx*—beam splitter; Mr_1, Mr_2, Mr_3—mirrors; *RFr*—Fresnel rhomb; *BS*—beam splitter; *SLM*—spatial light modulator HoloEye HEO-0017; DG_1, DG_2—digital phase grids; *D*—diaphragm; *A*—analyzer; G_1, G_2—phase gratings with distance Z_0=50 mm between them, *L*—Fourier-lens; *CCD*—a camera; PC_1 and PC_2 —computers; I_{s0}, I_{p0} with 2θ angle between them and I_0 are the input intensities; I_s^{out} and I_p^{out} are the output intensities

in the range of [0-π] allow us to produce the beam I_{s0} with a given change in intensity. The another beam I_{p0} which is generated by DG_1, possesses a stable intensity. *CCD* camera with a lens *L* register the output intensities of both beams, I_s^{out} and I_p^{out}. In these experiments on changing the signal intensity using SLM, we have revealed that the both outgoing beams, I_{s0} and I_{p0}, do not change their phase under any modulations of DG_1 and DG_2.

The experimental set-up shown in the Fig. 5 was also used to record holographic gratings, which formed *TDG*. Holographic plates (VRL-2) were placed sequentially in the P_r plane for exposure by a light interference pattern formed by beams with the same intensities $I_{p0} = I_{s0}$. After light exposure, the plates were developed and bleached. Changing the exposure time, the plates recorded different bright contrast, which after processing gave different modulation depths of the holographic gratings. All gratings have the same period $\Lambda = 22\ \mu$m and thickness of $d = 18 \pm 3\ \mu$m.

The above scheme was used to register the intensity spectrum of diffraction orders to define the modulation depth of fabricated gratings. To register the intensity spectrum formed by an individual grating, we use a mirror Mr_3 and a beam I_0, which propagated through the phase grating, as well as the lens *L* and *CCD* connected with *PC*. An experimental intensity spectrum generated by a grating was compared to the theoretically calculated spectrum (see our works [23, 24]). In this manner, we finally selected four gratings, G_1, G_2, G_3, G_4, with following experimentally defined phase delays: $\Phi_1 = 1.5$, $\Phi_2 = 1.465$, $\Phi_3 = 0.355$ and $\Phi_4 = 0.25$ rad. In the *TDG* design, one can change the modulation depths of the two gratings and the distance between them. We have developed two *TDG* that have similar modulation

Table 1 The elements of two different *TDG*s used in the experiment

Notation *TDG*	Gratings	Φ, rad	Z_0, mm
TDG_1	$G_1 : G_2$	1.5 : 1.465	50
TDG_2	$G_3 : G_4$	0.355 : 0.25	50

depths for both gratings and whose characteristics are given in Table 1.

We have studied the change in intensities in two main diffraction orders due to diffraction of two input coherent beams on the *TDG* depending on the input intensity ratio I_{p0}/I_{s0}. At the beginning of each experimental measurement, equal input intensities $I_{p0} = I_{s0}$ were set, and we adjusted the shift δ of the *TDG* relative to the interference pattern to achieve the maximum value of the energy transfer. In the Fig. 6 we present the typical output intensity spectrum detected at the *CCD* for equal input intensities, where we show the direct energy transfer from the pump beam to the signal beam (a), and the reverse energy transfer from the signal beam to the pump (b). After adjusting the maximum value of the energy transfer for the case of $I_{p0} = I_{s0}$, we started to control a phase modulation of the signal beam in the SLM, which causes a decrease in I_{s0}.

The experimental results of the energy transfer in the dependency of the input intensity ratio are presented in Fig. 7 for the TDG_1 (Fig. 7-I), and for the TDG_2 (Fig. 7-II). There we show the normalized values of the output intensities, I_p^{out}/I_0 and I_s^{out}/I_0 for the direct energy transfer (graphs (I-a), (II-a)), for the reverse energy transfer (graphs (I-b), (II-b)), and normalized input intensities, I_{p0}/I_0 and I_{s0}/I_0 (graphs (I-c), (II-c)), where $I_0 = I_{s0} + I_{p0}$.

It can be seen that for TDG_1 (Fig. 7-I), which contains gratings with strong modulation depths, the signal beam is amplified by a pump beam even under a strong decrease in the input signal. In case of reverse energy transfer at the

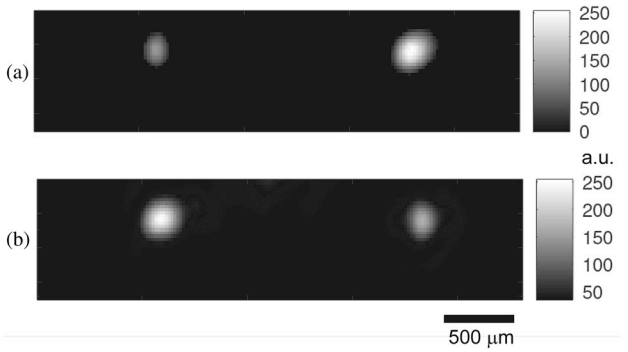

Fig. 6 Pictures of energy transfer recorded on a *CCD* for the case of equal input intensities. **a** Direct energy transfer, that is, the signal beam is amplified (right spot). **b** Reverse energy transfer, that is, the pump beam is amplified (left spot)

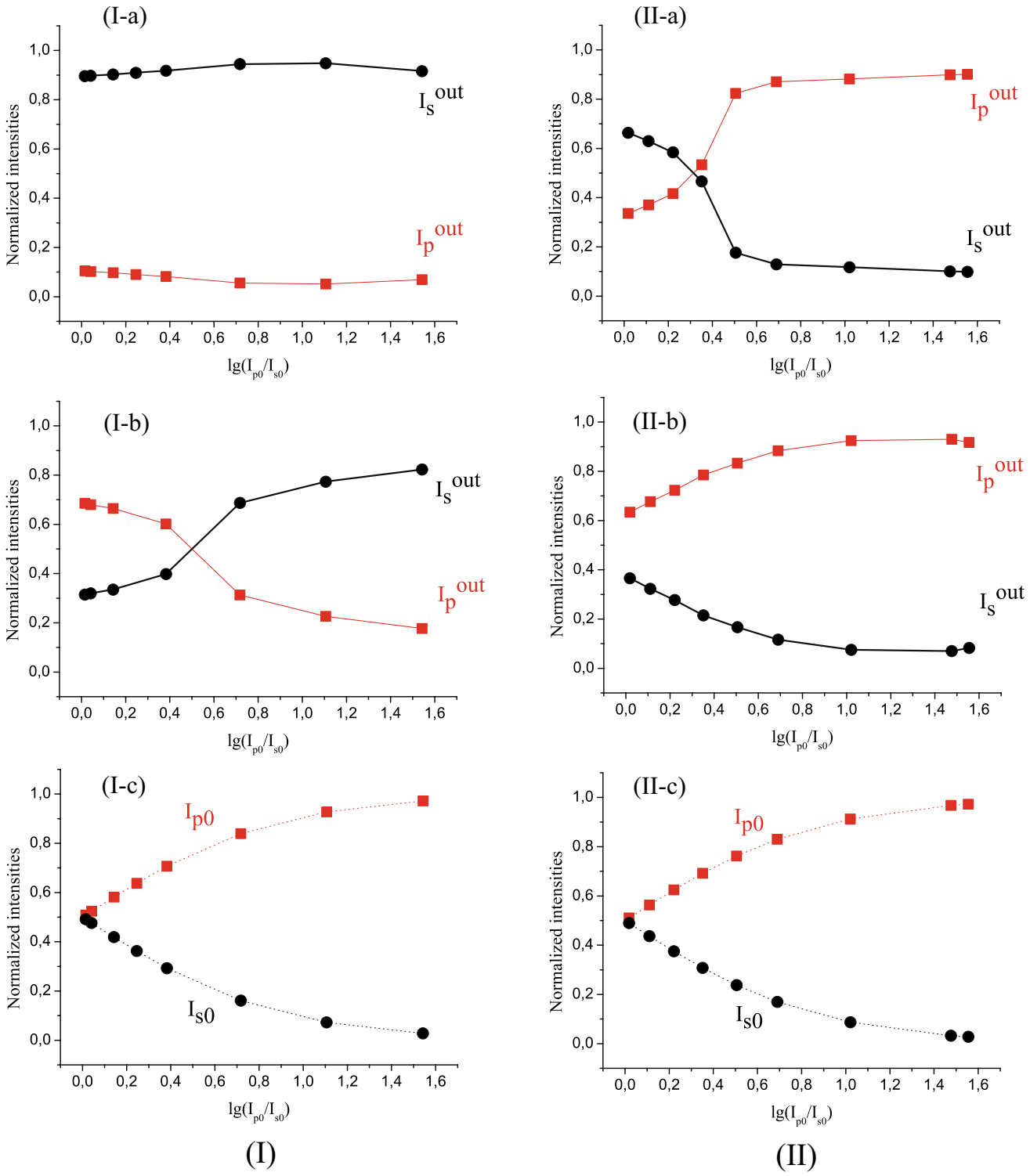

Fig. 7 Experimental energy transfer in TDG_1 (consisting of gratings with strong modulation depths)—I, and TDG_2 (consisting of gratings with weak modulation depths)—II, depending on the input intensity ratio: **a** direct energy transfer, **b** reverse energy transfer, **c** input intensities. Black marks for the signal beam, red marks for the pump beam. (Lines are only for visualisation)

beginning, Fig. 7(I-b), the direct energy transfer is restored with decreasing input signal intensity, and the signal beam again becomes amplified.

But for TDG_2, which consists of gratings with weak modulation depths, the situation is vice versa. In this case, the amplifying beam is the pump beam. With decreasing the input signal intensity, the output signal is reduced (Fig. 7-II).

The real experimental values of the intensities obtained in our set-up were as follows. The input intensity of the pump beam did not change, and its measured value was $I_{p0} \approx 240$ a.u. for TDG_1 and $I_{p0} \approx 250$ a.u. for TDG_2. At the same time, the input intensity of the signal beam was decreased, the measured values of I_{s0} were in the range $I_{s0} \approx 240...7$ a.u.. For the output signal beam in the scheme with TDG_1, we obtained an increase in the intensity of the smallest input signal by more than 20 times for both cases of direct $+U_d$ and reverse $-U_d$ energy transfer; the absolute value reached ≈ 160 a.u. Simultaneously, the output pump beam dropped to a value of ≈ 30 a.u. But for TDG_2, the smallest signal increased only by 10–20 a.u. in the case of a direct energy transfer; and for a reverse energy transfer, it slightly decreased or did not change.

In addition, in our experiments, we observed that under the condition of maximum energy transfer, the total energy is almost completely concentrated in two main diffraction orders with the smallest part scattered in high diffraction orders. Thus, in our case, the *TDG* system works similarly to one thick Bragg grating, despite the fact that the *TDG* includes thin gratings. We confirm this important finding in our further theoretical modeling.

5 Theoretical modeling of energy transfer in *TDG*

In this section we show that the Bragg diffraction of two coupled waves on the *TDG* can be described analytically on the base of coupled-wave theory. To apply the coupled wave model, we can approximate *TDG* as a bulk medium Z_0 thick, on the boundaries of which there are thin phase gratings G_1 and G_2, and they determine the boundary conditions for the grating amplitude. We assume the bulk medium contains one thick phase grating G_{SMG}. The modulation depth of the thick grating G_{TDG} is denoted by $\gamma_{\mathbb{N}}$. We can determine the value of $\gamma_{\mathbb{N}}$ from the assumption that the total phase delay, $\boldsymbol{\Phi}_{TDG}$, which the wave would receive due to diffraction by one thick grating G_{TDG}, should be equal to the sum of the phase delays, $\boldsymbol{\Phi}_1$ and $\boldsymbol{\Phi}_2$, that the wave would receive by diffraction on each of thin gratings G_1 and G_2, forming the *TDG*. Thus, $\boldsymbol{\Phi}_{TDG}$ satisfies the following relation:

$$\boldsymbol{\Phi}_{TDG} = \gamma_N k Z_0 = \boldsymbol{\Phi}_1 + \boldsymbol{\Phi}_2 \tag{12}$$

$$\boldsymbol{\Phi}_{1,2} = \Delta n_{1,2} \cdot kd \tag{13}$$

where Δn_1 and Δn_2 are the modulation depths of the corresponding thin gratings (that is, the maximum deviation of the refractive index of the grating from its average value n_0 ($n = n_0 + \Delta n$)); d is the thickness of a thin grating. The phase delay is an integral of the grating amplitude along the thickness within the boundaries of the medium multiplied by k.

We performed theoretical calculations of energy transfer using the formulas (9)–(11) for the schemes containing TDG_1, TDG_2, and for such input intensity ratio as in experiment. To do this, we needed to determine the parameters γ_N and q, which correspond to the characteristics of the *TDG*s. The value of γ_N is calculated by the ratio (12). The value of C is obtained from (5) using the input intensities: $C = \sqrt{I_{s0}^2 - I_{s0}I_{p0} + I_{p0}^2}/I_0$. The parameter q determines the offset of the maximum of the amplitude profile of the grating $N(z)$ relative to the origin. Since we assume that thin gratings are located at the boundaries z_1 and z_2, this parameter can be found by constructing the function $N(z)$ by the formula (6) with the boundary conditions: $[N(z_1);N(z_2)] = [\boldsymbol{\Phi}_1;\boldsymbol{\Phi}_2]$. In Table 2 we have collected all the parameters, γ_N and q, which correspondent to real *TDG*s, to carry out theoretical calculations.

Theoretical calculations for two different *TDG*s using experimental intensities for input beams are shown in the Fig. 8. The obtained theoretical graphs are in very good agreement with the experimental data (Fig. 7). Thus, these calculations, based on a model developed for a thick Bragg grating, confirm that *TDG* fulfills the coupling of two beams with the Bragg diffraction conditions.

6 Conclusion

We have demonstrated both experimentally and theoretically that two matched phase gratings separated by a space layer (the so-called *TDG* is a thick dual-grating) can work as one volume Bragg grating. When the *TDG* is illuminated by two coherent laser beams that form a light interference pattern, their diffraction by the *TDG* results in predominant energy transfer between two Bragg diffraction orders provided there is a shift δ of the interference pattern relative the *TDG* in the transverse direction. To calculate the maximum energy

Table 2 The parameters used to calculate the energy transfer in the *TDG* in accordance with the formulas (9)–(11)

TDG	γ_N	q	z_1, mm	z_2, mm
TDG_1	$5.97 \cdot 10^{-6}$	0	−25	25
TDG_2	$1.2 \cdot 10^{-6}$	−1.0	−25	25

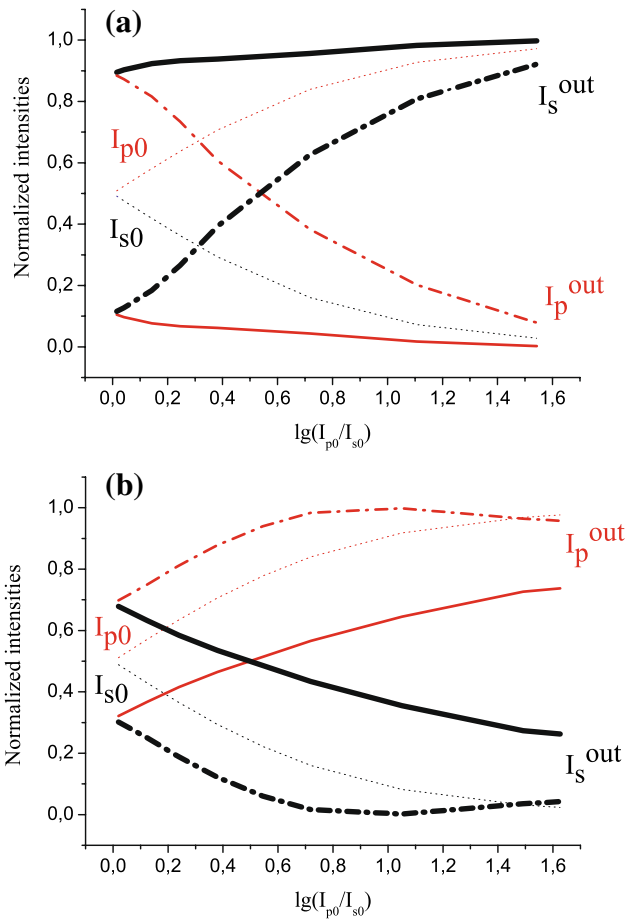

Fig. 8 Calculation of energy transfer between two main diffraction orders using the formulas (9)–(11) for experimental input intensity ratios (according to Fig. 7) and *TDG*s (Table 1); solid lines for $+U_d$ —direct energy transfer, dash-and-dot lines for $-U_d$—reverse energy transfer, dotted lines for the input intensities; **a** TDG_1; **b** TDG_2. Black lines for the signal beam, red lines for the pump beam

transfer in the *TDG* we have developed analytical model that is based on coupled wave theory (see Sects. 3 and 5).

When both grating in *TDG* have a small modulation depth, the classical effect of wave coupling takes place, the same as in a bulk medium with nonlocal optical nonlinearity. That is: direct energy transfer from the pump beam to the signal beam when the spatial shift $\delta = \Lambda/4$; and reverse energy transfer from the signal beam to the pump beam for the spatial shift $\delta = -\Lambda/4$. This spatial shift can be achieved by adjusting the phase difference between the two input laser beams.

We have discovered a new mode of unidirectional energy transfer for the case when both gratings in the *TDG* have a large modulation depth. Then there is only direct energy transfer to amplify the weaker beam by the stronger pump beam, regardless of the direction of the spatial shift δ. This mode was obtained for *TDG* both experimentally and theoretically, and it was not known for nonlinear photorefractive media.

Thus, our studies open up prospects for using a set of periodic gratings spaced at some distance, for a significant increase in intensity in an individual diffraction order, using all-optical methods: by changing the ratio of the input intensities of beams or/and modulation of the phase of one of the beams. The proposed holographic amplifier, in a simple and natural way, allows it to be adapted to a four-wave mixing scheme to creation optical phase conjugation (OPC) with unprecedented amplification of the OPC-beam. The advantages of this scheme are a high gain for weak laser beams in combination with the ability of image amplification when using a nonlinear medium instead of one of the grating, as well the simplicity of manufacturing *TDG* by laser engraving in a single monoblock.

Acknowledgements The authors gratefully acknowledge support from the Projects of the National Academy of Sciences of Ukraine B/197, 1.4.BC/185 and 25/18-H.

References

1. W.R. Boyd, *Nonlinear Optics* (Academic Press, Boston, 2003)
2. J. Hansryd, P.A. Andrekson, M. Weslund, J. Li, P.-O. Hedervist, Fiber-based optical parametric amplifiers and their applications. IEEE J. Sel. Top. Quantum Electron. **8**(3), 506–520 (2002)
3. A.P. Cracknell, L. Hayes, *Introduction to Remote Sensing*, 2nd edn. (Taylor and Francis, London, 2007)
4. A. Brignon, J.-P. Huignard (eds.), *Phase Conjugate Laser Optics* (Wiley, New York, 2004)
5. L. Lombard, A. Brignon, J.-P. Huignard, E. Lallier, P. Georges, G. Lucas-Leclin, G. Pauliat, G. Roosen, Review of photorefractive materials: an application to laser beam cleanup. C.R. Phys. **8**, 234–242 (2007)
6. I.P. Kaminow, T. Li, A.E. Willner (eds.), *Optical Fiber Telecommunications VIA Components and Subsystems* (Elsevier Science, Burlington, 2013)
7. A. Takada, W. Imajuku, Coherent optical amplifier. Rev. Laser Eng. **29**, 599–604 (2001)
8. P. Gunter, J.P. Huignard, *Photorefractive Materials and their Applications, 1, 2, and 3* (Springer, New York, 2006)
9. Jaime Frejlich, Photorefractive Materials, *Fundamental Concepts* (Wiley-Interscience, Hoboken, 2007)
10. A. Authier, *Dynamic Theory of X-way Diffraction* (Oxford University Press, Oxford, 2001)
11. P.P. Ewald, Crystal optics for visible light and X-rays. Rev. Mod. Phys. **37**(1), 46–56 (1965)
12. J.M. Cowley, *Diffraction Physics* (North-Holland, Amsterdam, 1975)
13. S. Savo, E. Di Gennaro, C. Miletto, A. Andreone, P. Dardano, L. Moretti, V. Micella, Pendellösung effect in photonic crystals. Opt. Express **16**(12), 9097–9105 (2008)
14. S. Dürr, S. Kunse, G. Rempe, Pendellösung oscillations in second-order Bragg scattering of atoms from a standing light wave. Quant. Semiclass. Opt. **8**(3), 531–540 (1996)
15. Maria L. Calvo, P. Cheben, O. Martinez-Matos, F. del Monte, J.A. Rodrigo, Experimental detection of the optical Pendelösung effect. Phys. Rev. Lett. **97**, 084801 (2006)
16. H. Kogelnik, Coupled wave theory for thick hologram gratings. Bell Syst. Techn. J. **48**(9), 2909–2947 (1969)

17. D.L. Staebler, J.J. Amodei, Coupled-wave analysis of holographic storage in LiNbO3. J. Appl. Phys. **43**, 1042–1049 (1972)
18. V. Kondilenko, V. Markov, S. Odulov, M. Soskin, Diffraction of coupled waves and determination of phase mismatch between holographic grating and fringe pattern. Opt. Acta **26**(2), 239–251 (1979)
19. B. Sturman, D.M. Giel, Description of readout process during strong beam coupling. Phys. Rev. E **69**, 066603 (2004)
20. S. Sturman, E. Podivilov, M. Gorkunov, Regimes of feedback-controlled beam coupling. Phys. Rev. E **72**, 016621 (2005)
21. A. Yariv, P. Yeh, *Optical waves in crystals* (Wiley and Son's, Inc., Hoboken, New Jersey, 2003)
22. K. Shcherbin, P. Mathey, G. Gadret, R. Guyard, H.R. Jauslin, S. Odoulov, Slowing down of light pulses using photorefractive four-wave mixing: non-trivial behavior with increasing coupling strength. Phys. Rev. A **87**, 033820 (2013)
23. S.A. Bugaychuk, V.O. Gnatovskyy, A.V. Sidorenko, I.I. Pryadko, A.M. Negriyko, Synthesis of dynamic phase profile by the correlation technique for spatial control of optical beams in multiplexing and switching. Proc. SPIE **9809**, 98090J (2015)
24. S.A. Bugaychuk, V.O. Gnatovskyy, A.M. Negriyko, I.I. Pryadko, Multiplication and commutation of laser beams under cross-correlation interaction of periodic fields. Ukr. J. Phys. **61**(4), 301–308 (2016)
25. M. Born, E. Wolf, *Principles of Optics* (Pergamon Press, Oxford, 1964)
26. M. Chi, J.P. Huignard, P.M. Petersen, A general theory of two-wave mixing in nonlinear media. J. Opt. Soc. Am. B **26**(8), 1578–1584 (2009)
27. M. Cronin-Collomb, B. Fisher, J.O. White, A. Yariv, Theory and applications of four-wave mixing in photorefractive media. IEEE J. Quantum Electron. **20**, 12–30 (1984)
28. A. Zozulya, V.T. Tikhonchuk, Investigation of stability of four-wave mixing in photorefractive media. Phys. Lett. A **135**, 447–450 (1989)
29. J.H. Hong, R. Saxema, Diffraction efficiency of volume holograms written by coupled beams. Opt. Lett. **16**, 180–182 (1991)
30. M. Jeganathan, M.C. Bashaw, L. Hesselink, Evolution and propagation of grating envelopes during erasure in bulk photorefractive media. J. Opt. Soc. Am. B **12**, 1370–1383 (1995)
31. S.A. Bugaichuk, A.I. Khizhnyak, Steady state and dynamic grating in photorefractive four-wave mixing. J. Opt. Soc. Am. B **15**(7), 2107–2113 (1998)
32. S. Bugaychuk, L. Kóvacs, G. Mandula, K. Polgár, R.A. Rupp, Nonuniform dynamic gratings in photorefractive media with nonlocal response. Phys. Rev. E **67**, 046603 (2003)
33. A.E. Miroshnichenko, S. Flach, Y.S. Kivshar, Fano resonances in nanoscale structures. Rev. Mod. Phys. **82**, 2257–2298 (2010)
34. A.E. Mirochnichenko, S.F. Mingaleev, S. Flach, Yu.S. Kivshar, Nonlinear Fano resonance and bistable wave transmission. Phys. Rev. E **71**, 036626 (2005)
35. A. Miroshnichenko, Y.S. Kivshar, Engineering Fano resonances in discrete arrays. Phys. Rev. E **72**, 056611 (2005)
36. R.D. Burioni, P. Sodano, A. Trombettoni, A. Vezzani, Topological filters and high-pass/low-pass devices for solitons in inhomogeneous networks. Phys. Rev. E **73**, 066624 (2006)
37. S. Bugaychuk, R.A. Rupp, G. Mandula, L. Kóvacs, Soliton profile of the dynamic grating amplitude and its alteration by photorefractive wave mixing. Trends Opt. Photons **87**, 404–409 (2003)